ARTICLES

Proton NMR Relaxation in Six-Coordinate Low-Spin Iron(III) Tetraphenylporphyrinates: Temperature Dependence of Proton Relaxation Rates and Interpretation of NOESY Experiments

Konstantin I. Momot and F. Ann Walker*

Department of Chemistry, University of Arizona, Tucson, Arizona 85721

The temperature dependence of longitudinal and transverse relaxation times (T_1 and T_2) has been studied for the pyrrole protons of $[(p\text{-Cl})_3(p\text{-NEt}_2)\text{TPPFe(III)}(N\text{-MeIm})_2]\text{Cl}$ (**1**), $[(p\text{-Cl})(p\text{-NEt}_2)_3\text{TPPFe(III)}(N\text{-MeIm})_2]\text{Cl}$ (**2**), and $[\text{TMPFe(III)}(2\text{-MeImH})_2]\text{Cl}$ (**3**), where TMP = tetramesitylporphyrin and TPP = tetraphenylporphyrin, in the temperature range 190−310 K. All three complexes are paramagnetic and have electron spin $S = \frac{1}{2}$. Up to 273 K, all complexes exhibit four distinct pyrrole proton signals, with the asymmetry caused by unsymmetrical substitution in complexes **1** and **2** and by axial ligands fixed in a definite orientation in complex **3**. Above 273 K the four-peak pattern in complex **3** collapses into a single peak due to fast synchronous rotation of axial ligands. At low temperatures, T_1s and T_2s in all complexes increase as temperature increases. At higher temperatures, T_1s continue to increase and equalize in complex **3**, but decrease in complexes **1** and **2**. T_2s in complexes **1** and **2** mimic the T_1s at all temperatures. In complex **3**, T_2s decrease as the four-peak pyrrole proton pattern collapses and increase again when the collapse is complete. This behavior has been attributed to chemical exchange induced by the rotation of 2-methylimidazole ligands. In complexes **1** and **2**, the decrease in both T_1s and T_2s at high temperatures is attributed to equilibrium between low-spin and high-spin complexes induced by dissociation of imidazole ligands in the TPP complexes. In all complexes, T_2s are considerably shorter than T_1s. Relaxation times in the TMP complex are generally larger than the corresponding values for the TPP complexes. The temperature dependence of the chemical shift follows the Curie law in complex **3** and is close to Curie behavior in complexes **1** and **2**, with slight deviations at high temperatures in the two latter complexes attributed to the low spin−high spin equilibrium. The NOE buildup curve for the pair of NOE-exhibiting pyrrole protons of complex **3** has been measured; the rate of NOE buildup has been found to be consistent with theoretical prediction based on the Stokes-estimated rotational correlation time and interproton distance measured from the MM2-minimized structure. A method has been proposed to predict the detectability of the NOE between a pair of structurally rigid protons in similar complexes, as well as to predict optimum detection conditions. Contrary to previous studies, no NOE is detected between pyrrole protons of **1** and **2**, and this fact is justified and discussed in light of our findings for complex **3**.

Introduction

1D and 2D ^{1}H NMR spectroscopy has proven an effective method for studying paramagnetic model hemes. A wide variety of structural and electronic information about metalloporphyrin complexes can be obtained, including spectral assignment using 2D spectroscopy,[1−4] rotational behavior of axial ligands studied by 1D and 2D NMR,[5−8] and the energy of low-lying electronic levels which can be derived from the temperature dependence of chemical shifts.[9] Several factors contribute to the great utility of ^{1}H NMR in such studies. One of them is that the metal paramagnetic center "illuminates" protons that are close to it, in that chemical shifts and relaxation times of such protons are largely determined by their spatial proximity to the paramagnetic metal and by how much unpaired electron density they bear. The second factor is the increased spectral resolution in areas containing paramagnetically shifted proton signals. In $S = \frac{1}{2}$ metalloporphyrin complexes, signals of protons that are closest to the metal atom can be spread over a region of several tens

of ppm. Although paramagnetic shifting also carries with it a sometimes significant increase in line width, resolution of resonances of paramagnetic compounds is usually superior to that of diamagnetic compounds due to less spectral crowding. Another factor is the strong temperature dependence of both chemical shifts and relaxation rates of paramagnetically shifted proton signals. Analysis of these dependences can potentially yield information about the factors contributing to both observables.

In paramagnetic compounds, the specifically paramagnetic sources of nuclear spin relaxation and nuclear chemical shift are multiple and are described in a number of textbooks and monographs.[10−12] Paramagnetic contributions to proton relaxation include dipole−dipole[13] and scalar (contact)[14] relaxation of proton spin due to the unpaired electron and Curie relaxation.[15] Even in low-spin ($S = \frac{1}{2}$) complexes, paramagnetic contributions to proton relaxation rates significantly exceed diamagnetic contributions (such as dipolar relaxation due to other nuclei and chemical shift anisotropy[16] relaxation) for protons that are close to the paramagnetic metal center.[11] The

paramagnetic contributions to the chemical shift can also be separated, to a first approximation.[17] The magnitude of the paramagnetic contributions to proton relaxation rate and chemical shift is very sensitive to the molecular geometry and electronic structure of the molecule. A change in either of these can lead to a significant change in relaxation rates and chemical shifts. Electronic aspects are especially important in metalloporphyrin complexes, because unpaired electron density is delocalized rather easily over the π-system of the porphyrin core and axial ligands. With that in mind, we have carried out a study of the temperature dependence of proton spin relaxation in several low-spin ($S = 1/2$) iron(III) porphyrin complexes. The ultimate goal of such a study is to experimentally determine the importance of each factor contributing to the relaxational behavior of the pyrrole protons. Pyrrole protons were chosen for study because the temperature dependence of their NMR parameters is particularly strong and because in all studied complexes their signals are well-resolved from each other and other signals in the spectrum.

The other contributor to the motivation for this study can be traced back to the work reported in ref 4. Two similar unsymmetrically substituted (tetraphenylporphyrinato)iron(III) complexes, [tris(*p*-chlorophenyl)(*p*-(diethylamino)phenyl)porphyrinato]iron(III) bis(*N*-methylimidazole) chloride, [(*p*-Cl)$_3$-(*p*-NEt$_2$)TPPFe(*N*-MeIm)$_2$]$^+$Cl$^-$ (**1**), and [(*p*-chlorophenyl)-tris(*p*-(diethylamino)phenyl)porphyrinato]iron(III) bis(*N*-methylimidazole) chloride, [(*p*-Cl)(*p*-NEt$_2$)$_3$TPPFe(*N*-MeIm)$_2$]$^+$Cl$^-$ (**2**), were studied in that work by means of 2D ^{1}H NMR spectroscopy (COSY and NOESY). In the NOESY spectra, one set of cross-peaks between pyrrole protons has been observed for one of the complexes, while two sets of cross-peaks have been observed for the other.[4] The source of such a difference was unclear at that time. In this work, we have attempted to investigate relaxation and cross-relaxation processes in these and another similar complex in hopes of understanding the origin of this phenomenon. The (tetramesitylporphyrinato)iron(III) bis-(2-methylimidazole) chloride complex, [TMPFe(2-MeImH)$_2$]$^+$Cl$^-$, **3**, has been chosen as a benchmark for this study for a number of reasons. Complex **3** is known to exhibit an NOE between one pair of pyrrole protons,[6,7] it has a size similar to those of **1** and **2**, and the chemical shifts of its paramagnetically shifted protons exhibit practically perfect Curie behavior.

In this paper, we discuss the experimentally observed temperature dependence of chemical shifts and longitudinal and transverse relaxation times in the three complexes. We also discuss our results regarding the NOESY spectra of complex **3** and their relevance to the other two complexes. We show how the temperature dependence of longitudinal relaxation times can be used to predict the optimal conditions for the detection of NOE. In particular, our work does not substantiate the existence of NOEs between pyrrole protons of complexes **1** and **2**, and we have shown theoretically that they cannot be observed in the solvent utilized in this and the earlier[4] study (CD$_2$Cl$_2$).

Experimental Section

1. Materials. Synthesis of unsymmetrically substituted iron-(III) tetraphenylporphyrinates has been described elsewhere.[18] Synthesis of chloroiron(III) tetramesitylporphyrinate utilized for this study has been described elsewhere.[19] *N*-Methylimidazole and 2-methylimidazole were purchased from Aldrich and used as received. A degassed sample of the bis(2-MeImH)-iron(III) tetramesitylporphyrinate chloride complex (**3**) with a slight excess of 2-MeImH was prepared in a 5 mm NMR tube in deuterated methylene chloride, CD$_2$Cl$_2$, purchased from Cambridge Isotope Laboratories, immediately prior to the recording

of spectra. Degassed samples of bis(*N*-MeIm)-iron(III) tetraphenylporphyrinates were prepared in 5 mm NMR tubes in CD$_2$Cl$_2$ ([(*p*-Cl)$_3$(*p*-NEt$_2$)TPPFe(*N*-MeIm)$_2$]$^+$Cl$^-$, **1**) or deuterated chloroform, CDCl$_3$ ([(*p*-Cl)(*p*-NEt$_2$)$_3$TPPFe(*N*-MeIm)$_2$]$^+$Cl$^-$, **2**), immediately prior to the recording of spectra.

2. One-Dimensional NMR Spectra. All spectra were recorded on a Bruker AM 500 spectrometer operating at 500.136 MHz for **1** and **2** and 500.138 MHz for **3**. The variable temperature control unit was calibrated using MeOH in the temperature range 195−295 K and using ethylene glycol in DMSO-d_6 in the range 295−310 K. All data relating to **3** were processed using Felix 2.30 for SGI workstation[20] as described below, except for the purposes of chemical shift measurements. All data relating to **1** and **2** were processed using the spectrometer's NMR software (DISNMR91)[21] as described below. Chemical shifts were measured using Felix or Bruker DISNMR software. Referencing of spectra was done by using the same parameter SR in the Bruker software, or by identically referencing the same spectral point in the Felix software, for all series of each given compound. The appropriate value of the spectral reference was found by referencing free 2-MeImH signals at 2.401 and 6.935 ppm or the free *N*-MeIm signal at 3.674 ppm at low temperatures (i.e., at the limit of no chemical exchange).

3. T_1 Relaxation Measurements. All spectra used for the measurement of T_1s were recorded using the standard inversion recovery pulse sequence.[22] For **3**, each temperature series contained 20 spectra with inversion recovery time ranging from 0.0001 to 0.3 s. Spectra were acquired with a spectral width of 20 000 Hz, 2K complex points, 80 transients per spectrum, 180° preparation pulse (13.2 μs), variable inversion recovery time, 90° detecting pulse (6.6 μs), followed by acquisition (typically 0.102 s) and relaxation delay of 1 s. Processing using Felix 2.30 included linear prediction of an additional 2K complex points (only in case of truncated data), Bruker Fourier transformation, and phasing, after which a region containing the pyrrole peaks was selected. The selected region was baseline corrected using Wüthrich's baseline flattening[23] or fifth-order polynomial correction when pyrrole peaks were very broad. Peaks were integrated to the corrected baseline level and their integrals were used to obtain the T_1 values using the least-squares fit utility of SigmaPlot 5.0.[24] A three-parameter fit ($I(t) = a_0 + a_1 e^{-t/T_1}$, where t is the variable inversion recovery time) was used for the least-squares fitting. Standard errors of the fitted T_1s (typically less than 1%) and reasonable closeness of the absolute values of the initial and final magnetization derived from the fit were used as criteria of the fit quality. For **1** and **2**, each temperature series also contained 20 spectra with inversion recovery time ranging from 0.0001 to 0.06 s. Spectra were recorded using typical spectral width of 3000 Hz to accommodate only the pyrrole peaks. The transmitter offset was adjusted as the peaks shifted downfield at lower temperatures. The spectrum size was 1K, with 40 transients per spectrum, 180° preparation pulse (16.6 μs), variable inversion recovery time, 90° detecting pulse (8.3 μs), followed by acquisition (0.171 s) and relaxation delay of 0.3 s. Processing using the DISNMR software included Fourier transformation, phasing, and automatic baseline correction. Peak heights were measured by the peak peaking command, and the heights were used in the least-squares fit procedure to obtain the values of T_1. The fitting procedure was the same as the one described for complex **3**.

4. T_2 Relaxation Measurements. The standard Hahn spin-echo pulse sequence was used in all cases for the determination of T_2 relaxation times.[25] For complex **3**, each temperature series

Iron(III) Tetraphenylporphyrinates

J. Phys. Chem. A, Vol. 101, No. 49, 1997 **9209**

contained 12 or 15 spectra with defocusing/refocusing time ranging from 0.0001 to 0.009 s or to 0.03 s, depending on the expected value of T_2 at a particular temperature. The same set of acquisition parameters was used as for the T_1 series of spectra. Processing using Felix 2.30 included linear prediction of truncated data, Bruker Fourier transformation, and phasing, after which the region containing pyrrole peaks was selected. The region of interest was baseline corrected using Wüthrich's baseline flattening procedure[23] or fifth-order polynomial baseline correction. Pyrrole proton signals were integrated to the corrected baseline level, and the integrals were used to obtain the values of T_2 by a three-parameter least-squares fit using SigmaPlot 5.0. The fit used was $I(t) = a_0 + a_1 e^{-2t/T_2}$, where t is the variable defocusing/refocusing time. Closeness of a_0 to zero and the magnitude of the standard error of T_2 (typically less than 1%) were used as criteria of the fit quality. For **1** and **2**, each temperature series contained 14 spectra with defocusing/refocusing time ranging from 0.0001 to 0.022 s. The same set of spectral parameters and the same processing were used as those for the T_1 spectra of the two compounds. The least-squares fitting procedure was identical with that described for T_2 spectra of **3**.

5. NOESY Spectra. A total of 12 NOESY spectra with mixing times ranging from 10 to 70 ms were used in constructing the NOE buildup curve of compound **3**. NOESY spectra were recorded using the standard phase-sensitive NOESY pulse sequence[26] at 191 K. The temperature was chosen so that no chemical exchange was observed between pyrrole protons and temperature equilibration was achievable within a reasonable length of time. The typical spectral parameters were as follows: spectral width 21 kHz, number of t_1 increments 512, 64 transients per increment, number of data points in t_2 2226. Processing was performed using Felix 2.30 and included, in the direct dimension, FID drift correction using the last 10% of the FID, zero-filling to 2K complex points, Gauss−Lorentzian apodization (gb = −1, lb = 0.018), Bruker Fourier transformation, phasing, cubic spline baseline correction, and discarding the imaginary part of the spectrum. In the indirect dimension, processing included zero-filling to 2K real points, Gauss−Lorentzian apodization (gb = −1, lb = 0.002), real Fourier transform, phasing, and discarding the imaginary part of the spectrum. When additional phase correction was necessary, it was done by performing a Hilbert transform, rephasing, and discarding the imaginary part of the spectrum again. The apodization method was chosen based on our observation that this type of apodization with window parameters close to those cited above does not significantly change the relative intensities of diagonal and cross peaks. Equality of integrals of the two cross peaks was used as a criterion of the overall quality of the spectra. After suitable spectra were obtained, the intensities of the two diagonal peaks from the pyrrole signals exhibiting the NOE and the two cross peaks between them were integrated to the level of the noise, and integrals were used to construct NOE buildup curve as described in the Data Analysis section.

Data Analysis

Transverse and longitudinal proton relaxation rates were determined using a standard three-parameter fit as described in the Experimental Section.

NOE Buildup Curve. For two protons interacting with each other only as magnetic dipoles the peak intensities in the NOESY spectrum are given by[27]

$$I_{AA} = e^{[-(R_A+R_B)/2]\tau_m}\left(e^{A\tau_m} + \frac{R_A + R_B - 2A}{2A}\sinh A\tau_m - \frac{R_A}{A}\sinh A\tau_m\right) \quad (1)$$

$$I_{BB} = e^{[-(R_A+R_B)/2]\tau_m}\left(e^{A\tau_m} + \frac{R_A + R_B - 2A}{2A}\sinh A\tau_m - \frac{R_B}{A}\sinh A\tau_m\right) \quad (2)$$

$$I_{AB} = I_{BA} = e^{[-(R_A+R_B)/2]\tau_m}\frac{R_{AB}}{A}\sinh A\tau_m \quad (3)$$

where

$$A = {}^1\!/_2[(R_A - R_B)^2 + 4R_{AB}^2]^{1/2} \quad (4)$$

and R_A and R_B are the relaxation rates of protons A and B, $R_{AB} = R_{BA} = W_0 - W_2$ is the rate of cross-relaxation of the two protons, W_i is the rate of an i-quantum transition in the two-spin system, and τ_m is the mixing time in the NOESY pulse sequence. The term $e^{[-(R_A+R_B)/2]\tau_m}$ describes the general relaxation of longitudinal magnetization and does not contain any NOE-specific information. It can be eliminated by using the relative cross-peak intensity,

$$I_R = \frac{I_{AB} + I_{BA}}{I_{AA} + I_{BB}} = \frac{R_{AB}}{A}\tanh(A\tau_m) \quad (5)$$

In the above expression, R_{AB}/A is a constant characterizing the system and independent of mixing time. It represents the maximum relative intensity of cross-peaks that can potentially be achieved. When the NOE is between two protons that have the same longitudinal relaxation time, the maximum potentially achievable relative intensity of cross-peaks is 1. The hyperbolic tangent in expression 5 starts at 0 at $\tau_m = 0$ and exponentially approaches 1 at long mixing times, which are longer than the τ_ms used in this study. In practice, the asymptotic intensity can almost never be detected, because at mixing times long enough to achieve it the longitudinal magnetization relaxes almost completely, and the intensity of all peaks is below the level of noise. At the other extreme, i.e., at "small" mixing times, the relative cross-peak intensity can be approximated as

$$I_R(\tau_m) = \tau_m R_{AB} = \tau_m(W_0 - W_2) \quad (6)$$

That is, the initial buildup of NOE is linear with respect to the mixing time, whether the two protons have the same rate of longitudinal relaxation. This fact greatly facilitates the interpretation of NOE buildup curves, because the cross-relaxation rate can be obtained via linear least-squares fit of the initial part of the NOE buildup curve. The term "initial" refers to short mixing time, which shall be defined as

$$\tau_m \ll \frac{1}{\left[\left(\dfrac{1}{T_{1A}} - \dfrac{1}{T_{1B}}\right)^2 + 4R_{AB}^2\right]^{1/2}} \quad (7)$$

For the particular system studied (NOE between pyrrole protons b and c of complex **3**) the value of the square root in eq 7 is approximately 1 s^{-1} at the temperature used to record the NOESY spectra. This means that mixing times of 0.1 s and smaller can be considered short for the purpose of approximating the NOE buildup curve by a straight line. In the NOE buildup

curve obtained in this work for compound **3**, the largest mixing time was 70 ms.

Transition rates W_0 and W_2 are proportional to the spectral densities of motion at their corresponding frequencies:[27]

$$W_0 = \frac{1}{2}q_{AB}J(\omega_{0A} - \omega_{0B})$$

$$W_2 = 3q_{AB}J(\omega_{0A} + \omega_{0B})$$

$$J(\omega) = \frac{2\tau_c}{1 + \omega^2\tau_c^2} \qquad q_{AB} = \frac{1}{10}\gamma^4\hbar^2 r_{AB}^{-6}\left(\frac{\mu_0}{4\pi}\right)^2 \quad (8)$$

where τ_c can be thought of as the molecular reorientation time. Setting $\omega_{0A} = \omega_{0B} = \omega_0$, we have

$$R_{AB} = (W_0 - W_2)\tau_m = \frac{1}{10}\gamma^4\hbar^2 r_{AB}^{-6}\left(\frac{\mu_0}{4\pi}\right)^2\left(\tau_c - \right.$$

$$\left. \frac{6\tau_c}{1 + 4\omega_0^2\tau_c^2}\right) \quad (9)$$

From eq 9, τ_c was found by equating the right-hand side of eq 9 to the experimentally measured value of R_{AB} (0.57 s^{-1}) and numerically solving the resulting equation for τ_c. The error margin for τ_c was determined by repeating the procedure for $R_{AB} - \sigma(R_{AB})$ and $R_{AB} + \sigma(R_{AB})$ and taking half of the absolute value of the difference between the two resulting τ_c values as $\sigma(\tau_c)$.

Results and Discussion

General Comments. (Tetramesitylporphyrinato)iron(III) bis-(2-methylimidazole) chloride, [TMPFe(III)(2-MeImH)$_2$]Cl (**3**), has a symmetric porphyrin core with mesityl groups in all four *meso*-positions of the porphyrin ring. Nevertheless, its eight pyrrole protons exhibit four distinct NMR signals in the temperature range 190−273 K (at 500 MHz field). It has been shown[5,6] that the cause of this asymmetry is that the unsymmetrical 2-methylimidazole axial ligands induce asymmetry, and they do not rotate sufficiently fast for the pyrrole protons to become equivalent on the NMR time scale. In the related crystal structure, the 1,2-dimethylimidazole axial ligands of the complex are orientated perpendicularly with respect to each other, bisecting the porphyrin nitrogens.[28] At low temperatures, the axial ligands slowly rotate, inducing chemical exchange between the different pyrrole positions but no averaging in ^{1}H NMR spectra. The rate of the rotation has been measured by various methods[5,7,29] in the temperature range 200−245 K. Above 273 K at 500 MHz, the four-peak pattern collapses into one broad peak around −10 ppm. The collapse is attributed to the fact that the rotation at that temperature is sufficiently fast to cause the complete exchange averaging of the signals from different types of pyrrole protons. The following estimate illustrates that the collapse is indeed due to the exchange. At 270 K, the average distance between different pyrrole proton signals is 2 ppm, which at 500 MHz field corresponds to 1000 Hz. Hence, the collapse of the pattern should begin when the exchange rate reaches 2000 s^{-1} ($k_{coalesc} = \Delta\omega/2\sqrt{2}$ for two peaks with no intrinsic relaxation). Thermodynamic parameters of rotation obtained in the previous studies (summary is given in ref 29) give the exchange rate constant at 273 K between 1400 and 4000 s^{-1} (which is sufficiently large to consider the exchange as intermediate) and between 12 000 and 46 000 s^{-1} at 300 K (fast exchange). Indeed, the pattern collapses just above 273 K at 500 MHz field strength. At the 300 MHz field strength, the collapse occurs at a lower temperature, approximately −10
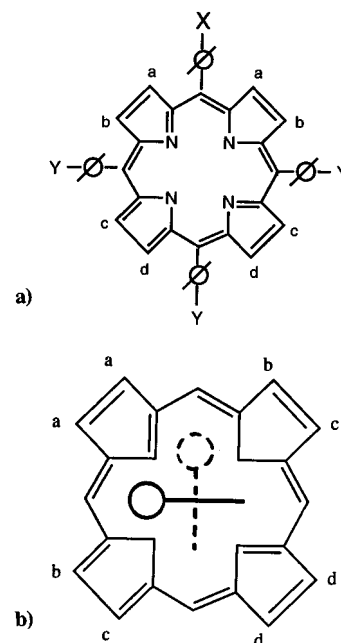
Figure 1. Four distinct pyrrole positions in (a) unsymmetrically substituted complexes **1** and **2** and (b) symmetrically substituted complex **3** with frozen axial ligands. In the former, the axial ligands are not shown because their fast rotation does not affect the asymmetry of the complex. Note that the symmetry and the labels of the pyrrole positions are different in the two cases. ^{1}H NMR spectra of the complexes and their assignment can be found in the literature.[4,6,7]

°C, where the exchange rate can be estimated between 580 and 1400 s^{-1}. This is consistent with the smaller (on the frequency scale) distance between the signals at the latter field strength.

Another evidence that the collapse of the four-peak pattern in complex **3** is caused by rotation of axial ligands and not by other phenomena, such as equilibrium between different spin states due to ligand exchange, is the observation that the collapsed peak is found in the same area as the peaks of the four-peak pattern, whereas a collapse due to low spin−high spin equilibrium would significantly shift the peak (as happens for complexes **1** and **2**).

[Tris(*p*-chlorophenyl)(*p*-(diethylamino)phenyl)porphyrinato]-iron(III) bis(*N*-methylimidazole), [(*p*-Cl)$_3$(*p*-NEt$_2$)TPPFe(*N*-MeIm)$_2$]$^+$ (**1**), and [(*p*-chlorophenyl)-tris(*p*-diethylamino)phenyl)-porphyrinato]iron(III) bis(*N*-methylimidazole), [(*p*-Cl)(*p*-NEt$_2$)$_3$-TPPFe(*N*-MeIm)$_2$]$^+$ (**2**), are structurally different from **3** in two ways. First, both complexes **1** and **2** contain unsymmetrically substituted porphyrin cores with three of the *meso*-positions carrying substituents of one type and the fourth *meso*-position carrying a substituent of a different type. Second, the axial ligands (*N*-methylimidazole) and peripheral substituents in these complexes are not as bulky as those in complex **3**, and the axial ligands rotate freely throughout the temperature range that extends down to at least 185 K. Because complexes **1** and **2** contain a unique substituent on their porphyrin ring, four distinct pyrrole positions are also present in these complexes, as in the case of complex **3** at low temperatures. However, the cause of the asymmetry is different in these two cases, and the asymmetry patterns are different for the two types of complexes. Figure 1 shows the unique pyrrole positions in the TMP complex and the two TPP complexes.

Because the axial ligands in complexes **1** and **2** rotate very fast at all temperatures that have been studied by us by means of ^{1}H NMR,[30] they do not introduce any additional asymmetry in these complexes, beyond that caused by the unsymmetrical substitution. Therefore, one can expect to observe four distinct

NMR signals from the pyrrole protons of **1** and **2** at all temperatures. Indeed, in the presence of excess of free *N*-methylimidazole both complexes exhibit four distinct pyrrole signals in the range of at least from 191 to 313 K. However, without an excess of *N*-methylimidazole being present, the four peaks collapse and reappear as one very broad (several ppm line width) peak around 80 ppm. This behavior has been attributed to equilibrium between the bis-ligated *N*-MeIm form, which has $S = \frac{1}{2}$ (low spin) electronic state, and the mono-ligated form, which has $S = \frac{5}{2}$ (high spin) electronic ground state.[31] This will be further discussed below in connection with proton chemical shifts and relaxation times in complexes **1** and **2**.

Chemical Shifts. Chemical shifts in many paramagnetic compounds obey the Curie law,[17] where the value of the "paramagnetic" part of the chemical shift is inversely proportional to the temperature:

$$\delta_{\mathrm{para}} = F/T \qquad (10)$$

where F is a factor unique to a particular proton (Curie factor).[32] In many compounds, the factor F has positive value for some peaks and negative value for other peaks.[33-37] In other compounds, including many metalloporphyrin complexes, NMR chemical shifts exhibit deviations from eq 10 in that the Curie plots may not be linear[38,39] or they are linear but show an unexpectedly large value of the intercept at zero inverse temperature ("anti-Curie" behavior).[33,35,36,40,41] It has been shown that both nonideal Curie and anti-Curie behavior can be explained by the second-order Zeeman effect and spin−orbit coupling[42,43] or by the presence of low-lying excited electronic states.[9,39,44-46] For the first-row transition-metal complexes, Curie behavior of chemical shifts is most likely an indicator of only one electronic state being populated.[9,46]

The temperature dependence of chemical shifts of pyrrole protons has been studied in the range 190−310 K for complexes **1**−**3**. The results are shown in Figure 2. When chemical shifts of pyrrole protons follow ideal Curie behavior, the infinite-temperature intercepts of their Curie plots should fall in the region 7−9 ppm. Complex **3** shows nearly perfect Curie behavior of the pyrrole signals at least as long as the four-peak pyrrole proton pattern is retained. All peaks have a linear dependence of their chemical shifts versus inverse temperature, and infinite-temperature intercepts are between 7 and 8 ppm for three of the peaks and 5 ppm for the fourth peak. This is consistent with the results of previous studies.[6] No definite deviations from the Curie behavior can be observed in this complex even after the four-peak pattern collapses.

Complexes **1** and **2** appear to follow the Curie law at low temperatures, although not as well as **3**. Their chemical shift intercepts are closer to 0 ppm when only the lowest temperature data are considered. At higher temperatures (250 K and above) the pyrrole proton signals of both complexes start to deviate from Curie behavior. As a result, the Curie plots for all pyrrole protons in complexes **1** and **2** are concave curves with the high-temperature ends having greater slope than the low-temperature ends.

These observations are consistent with the earlier conclusion[31] that an equilibrium between low-spin and high-spin forms is present in complexes **1** and **2** at high temperatures. Indeed, the two forms possess different distributions of electron spin density and have very different chemical shifts for the paramagnetically shifted protons. As was mentioned above, when the monoligated high-spin form is the dominant one, the pyrrole proton signal is observed in the vicinity of 80 ppm (room temperature), while the four pyrrole signals of the bis-ligated
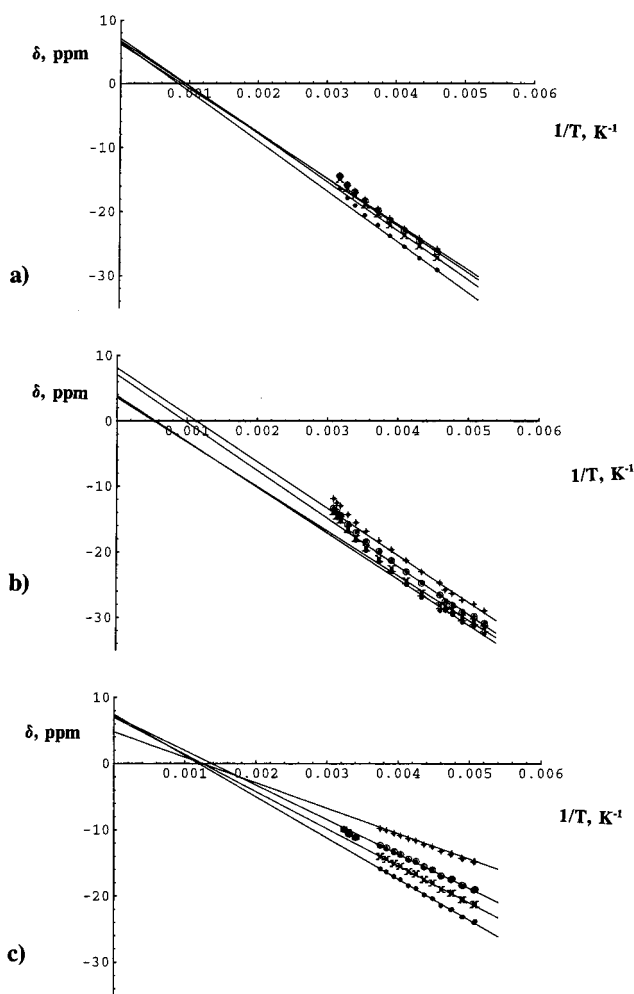
Figure 2. Temperature dependence of the chemical shifts of the four distinct pyrrole protons for (a) [(*p*-Cl)$_3$(*p*-NEt$_2$)TPPFe(III)(*N*-MeIm)$_2$]$^+$-Cl$^-$ (**1**), (b) [(*p*-Cl)(*p*-NEt$_2$)$_3$TPPFe(III)(*N*-MeIm)$_2$]$^+$Cl$^-$ (**2**), and (c) [TMPFe(III)(2-MeImH)$_2$]$^+$Cl$^-$ (**3**). Note the deviation from Curie behavior at high temperatures for complexes **1** and **2**.

low-spin form are observed between −10 and −30 ppm, depending on the temperature. As the temperature is increased, the fraction of the high-spin form also increases, thereby shifting the observed chemical shift toward that of the $S = \frac{5}{2}$ form. This is the result of the proximity of the ligand exchange to the intermediate mode, and it causes the chemical shifts to have greater values at high temperatures than would have been expected without the chemical equilibrium. In complex **3**, a similar chemical equilibrium exists, but there are no indications of it in our chemical shift data or, as will be seen below, in our relaxation times data. This observation is consistent with the fact that in complex **3** the binding constant of axial ligands, β_2, is greater than those in complexes **1** and **2**: 10^6 M^{-1} in the former and 10^3−10^4 M^{-1} in the latter. The low spin−high spin equilibrium probably would be observed at a higher temperature or under lower concentrations of free 2-methylimidazole (axial ligand).

Relaxation Times. Longitudinal (T_1) and transverse (T_2) relaxation times of pyrrole proton signals have been studied for all three complexes in the same temperature ranges as described for the chemical shifts. The results are shown in Figures 3 (T_1s) and 4 (T_2s). For complex **3**, longitudinal relaxation times uniformly increase with temperature throughout the temperature range studied. At low temperatures, T_1s for protons a, b, and c differ from each other by no more than 7% and can be considered almost equal. The T_1 for proton d is shorter than the other three T_1s by as much as 22%. However,

at higher temperatures the T_1s of the four signals equalize, until they eventually collapse into one exchange-averaged signal.

At low temperatures, transverse relaxation times are generally 65–90% shorter than the corresponding longitudinal relaxation times. Transverse relaxation times for all four protons increase with temperature in the range 190–230 K. The decrease of the T_2s, occurring in the temperature range 230–295 K, coincides with the collapse of the four-peak pattern.

The behavior of proton relaxation rates in complex **3** is consistent with the presence of the following two trends that govern the change of transverse[47] and longitudinal[48] relaxation rates with temperature: (i) intrinsic relaxation times of all four pyrrole protons increase with temperature, which is manifested by the fact that the average and individual T_1s increase throughout the studied temperature range; (ii) at the higher temperatures, the observed relaxation times are modified by chemical exchange. Transverse relaxation times in this range significantly differ from the intrinsic values. Unlike in complexes **1** and **2**, chemical shifts are not modified by chemical exchange in complex **3**. The exchange in the latter involves peaks with similar chemical shifts, and exchange shifting of signals is apparently marginal in the slow exchange limit.

In a separate study,[49] we demonstrate that the behavior of the T_2s in complex **3** is not only qualitatively consistent with these conclusion but can also be interpreted quantitatively in order to determine the rate constant of the four-site cyclic exchange.

The shortening of T_1s at high temperature in complexes **1** and **2** therefore suggests that an equilibrium is present with a form that has significantly shorter intrinsic T_1s and that at higher temperatures the rate constant of the forward reaction of such equilibrium is large enough to cause the shortening of the observed T_1s of the pyrrole protons in the low-spin form. As chemical shift data suggest, the equilibrium in question is between bis-ligated (low-spin) and mono-ligated (high-spin) forms of complexes **1** and **2**. The relaxation rates of the pyrrole protons in the high-spin form have not been measured, but their T_2s should be assumed to be 1–2 ms, judging from the line width of the pyrrole signal in the high-spin form.[50] Since chemical exchange equalizes longitudinal relaxation times even before the exchanging peaks start collapsing, slow chemical exchange with a high-spin state significantly shortens T_1s. Numerical simulations of complexes **1** and **2** do not appear promising in the quantitative sense, because they would involve too many degrees of freedom (forward and reverse rate constants and concentration of the free ligand). However, the shortening in T_1s in these complexes is qualitatively consistent with the presence of such equilibrium.

The conclusion of this section that is of an immediate practical importance to this paper is that only relaxation rates at the lower temperatures (190–230 K for **3**, 215–270 K for **1** and **2**) are representative of the intrinsic relaxation rates, while at higher temperatures all observed relaxation rates are modified by chemical exchange. For this reason, only the lower temperature relaxation data are meaningful for interpretation in the context of the complexes' electronic structure. The same is true for the chemical shifts, although the effect of chemical exchange on chemical shift at 270 K is more pronounced in complexes **1** and **2** than it is in complex **3**.

The other important conclusion of this section is that, since proton relaxation times in paramagnetic complexes are largely determined by the relaxation times of the unpaired electron (T_{1e} and T_{2e}),[12] their temperature dependence in the temperature range 190–250 K can potentially yield valuable and otherwise unattainable information about the mechanisms and the relevant
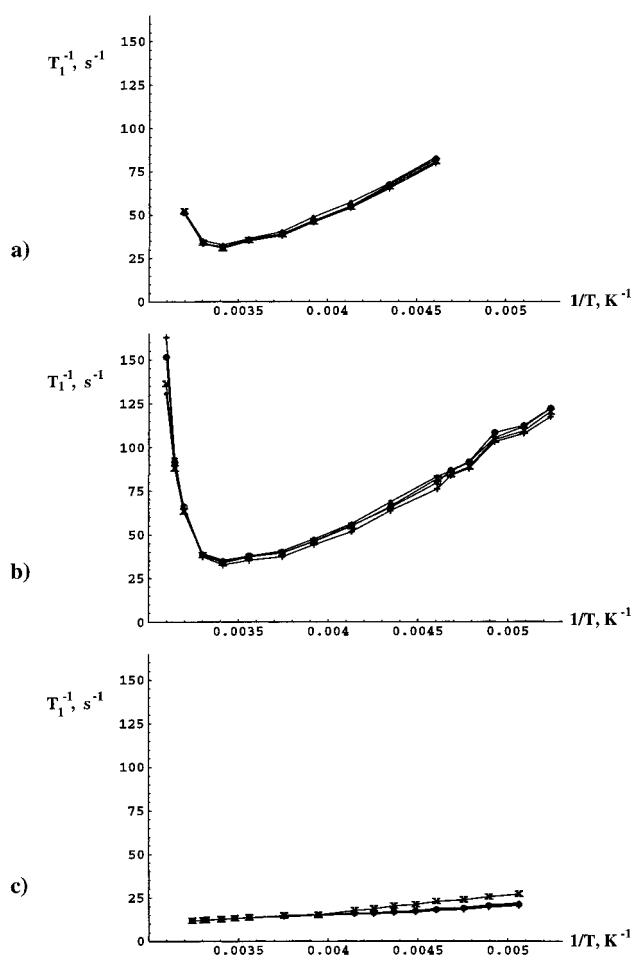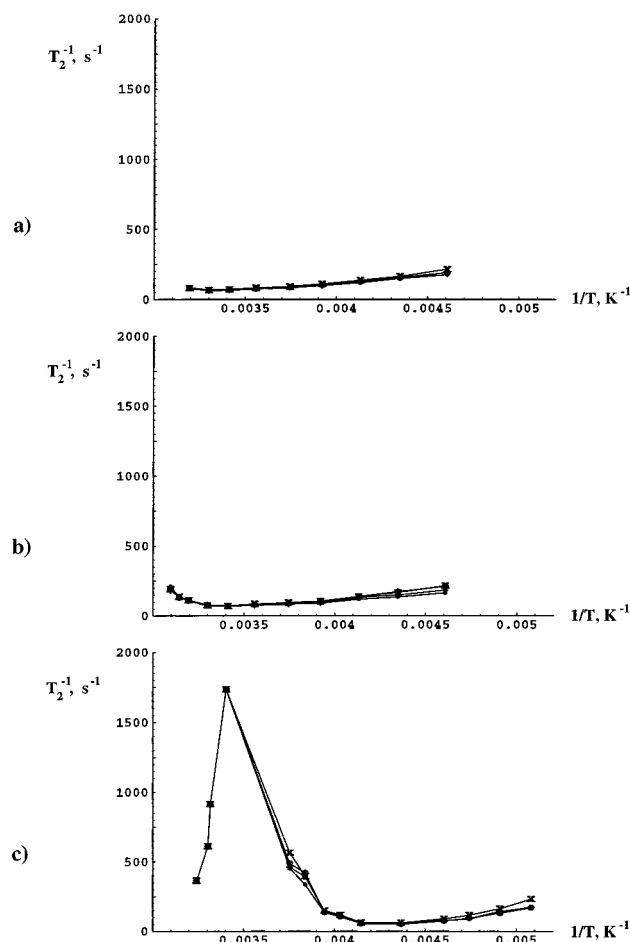

Figure 3. Temperature dependence of the longitudinal relaxation times (T_1) of the four distinct pyrrole proton signals for (a) [(p-Cl)$_3$(p-NEt$_2$)TPPFe(III)(N-MeIm)$_2$]$^+$Cl$^-$ (**1**), (b) [(p-Cl)(p-NEt$_2$)$_3$TPPFe(III)-(N-MeIm)$_2$]$^+$Cl$^-$ (**2**), and (c) [TMPFe(III)(2-MeImH)$_2$]$^+$Cl$^-$ (**3**). Note that T_1s decrease at high temperatures for complexes **1** and **2**, but not for complex **3**.

parameters of high-temperature electronic relaxation in low-spin iron(III).[12,51] This will be the subject of a separate study.

NOE Buildup Curve for Complex 3. NOESY spectra for complex **3** were reported several years ago.[6] At −74 °C, a 300 MHz NOESY spectrum exhibits only cross-peaks between spatially close protons. At that temperature, pyrrole protons a and b exhibit NOE cross-peaks with protons of *ortho*-methyl 3 (see Figure 4, ref 6), while pyrrole protons c and d show cross-peaks with protons of *ortho*-methyl 2. Also, a set of cross-peaks between pyrrole protons b and c is observed. The data were used to make signal assignments in the ^{1}H spectra of the complex. At higher temperatures (−54 and −29 °C), an exchange pattern appears between the four pyrrole peaks and between the four *ortho*-CH$_3$ peaks (see Figures 1 and 2, ref 6). This, as well as the temperature dependence of cross-peak intensities, has been interpreted as the presence at the higher temperatures of a four-site exchange induced by slow collective rotation of the two 2-methylimidazole ligands. Similar results have been recently obtained from NOESY and ROESY experiments.[7,8] In the latter, slow-rotation-limit NOE and exchange cross-peaks have different signs,[52] thus providing an independent confirmation of the cross-peak origins. The rate of rotation of the 2-methylimidazole ligands has also been determined from the intensities of the diagonal and cross-peaks at a number of temperatures.[7]

In the current work, we used the phase-sensitive NOESY technique with complex **3** at a temperature (191 K) where the

Iron(III) Tetraphenylporphyrinates

J. Phys. Chem. A, Vol. 101, No. 49, 1997 **9213**

Figure 4. Temperature dependence of the transverse relaxation times (T_2) of the four distinct pyrrole proton signals for (a) $[(p\text{-Cl})_3(p\text{-NEt}_2)\text{TPPFe(III)}(N\text{-MeIm})_2]^+\text{Cl}^-$ (**1**), (b) $[(p\text{-Cl})(p\text{-NEt}_2)_3\text{TPPFe(III)}(N\text{-MeIm})_2]^+\text{Cl}^-$ (**2**), and (c) $[\text{TMPFe(III)}(2\text{-MeImH})_2]^+\text{Cl}^-$ (**3**).

characteristic four-peak chemical exchange pattern was not present. The goal was to measure the NOE cross-peak intensity without contribution from chemical exchange and to construct the buildup curve for the NOE between pyrrole protons b and c. These protons were chosen because they exhibit the only set of NOE cross-peaks where the participating protons are structurally rigid. Protons from at least one methyl group participate in all other NOEs present in this complex, meaning that the rapid rotation of the methyl group and possibly libration of the mesityl ring have to be taken into account in order to correctly interpret the peak intensities in a quantitative way. This complication is not present when the NOE in question is between two pyrrole protons.

NOESY spectra were recorded at a number of different mixing times, ranging from 10 to 70 ms. The number of transients and t_1 increments in the spectra varied, but the external experimental conditions were the same (500 MHz, $T = 191$ K (-82 °C), no spinning of the sample). The intensity of the cross-peaks in each case was expressed in terms of the relative cross-peak intensity as described in the Data Analysis section. The use of unitless relative intensities not only simplifies the quantitative interpretation (at short mixing times, there is a linear relationship between I_R and τ_m that is invariant to the proton relaxation times) but also allows comparison of the results from two different experiments with different sample concentrations, different number of t_1 increments or t_2 transients, etc. A plot of the relative cross-peak intensity against mixing time is shown in supporting Figure S1, along with the linear best fit to the data. The best fit line has a small nonzero intercept, which

TABLE 1: Dynamic Data Obtained from the Measurements of NOE Buildup between Pyrrole Protons b and c in $[\text{TMPFe(III)}(2\text{-MeImH})_2]^+\text{Cl}^-$ (3) at -82 °C

R_{AB}, s^{-1}	$\sigma(R_{AB})$,[a] s^{-1}	τ_c, s	err,[b] s
0.57	0.10	3.3×10^{-9}	0.5×10^{-9}

[a] Standard error of the linear regression procedure. [b] Calculated as half the absolute value of the difference between the two τ_c values found from $R_{AB} + \sigma(R_{AB})$ and $R_{AB} - \sigma(R_{AB})$.

probably reflects the residual baseline imperfections and contributions from t_1 noise, while the slope is the absolute value of the rate of NOE cross-peak buildup.

The plot in supporting Figure S1 definitely shows an increase of cross-peak relative intensity with the mixing time, although the deviation of some of the experimental points from the fitting line is significant. Therefore, error analysis should be given proper attention in attempts to quantitatively interpret the data. First of all, although the error is significant, its nature is random rather than systematic, in that the deviating data points do not suggest curvature but are symmetrically distributed around a straight line throughout the mixing time range. Therefore, the error is not associated with a possible violation of the short mixing time approximation. Second, no four-site chemical exchange pattern between pyrrole or *ortho*-CH$_3$ protons is present in the NOESY spectra even at large mixing times, as can be seen from supporting Figure S2. Lowering the contour levels to the level of noise does not reveal any cross-peaks that are not seen in that Figure. Further, the previous measurements of exchange activation parameters[5,7,29] yield the upper estimate for the exchange rate at -82 °C between 0.04 and 0.06 s^{-1}, which is an order of magnitude smaller than the measured rate of NOE buildup (shown in Table 1). Therefore, we conclude that it is not possible at that temperature for chemical exchange contributions to significantly distort the intensities of NOE cross-peaks. This leads us to believe that the error originates in two factors, namely, poor baseline and strong t_1 noise. Although our best efforts have been made to adequately correct the baseline in each spectrum, the large dynamic range of the spectra makes it almost impossible to perform the correction so that the baseline deviations would be low enough as to not distort the intensity of the NOE cross-peaks (which have the lowest intensity among all peaks in the spectrum). One evidence of baseline imperfections was obtained when we tried to vary the integration area from "the baseline level" to integrating to half-distance between neighboring peaks. Increasing the integration area led to serious changes in the measured peak volumes, sometimes yielding negative intensities for positive cross-peaks (as a result of negative baseline deviation) and other times yielding a positive intensity significantly larger than integration to the baseline level (as a result of positive baseline deviations). Thus, integration "to the baseline level" was chosen as a compromise so as to exclude the baseline deviations outside of the cross-peak from the measured intensity. However, it is clear that some baseline deviations within the peak area remain and affect the measured intensity.

Another evidence of t_1 noise and poor baseline being the primary sources of error is the sometimes significantly unequal relative intensity of the two individual cross-peaks, $2I_{AB}/(I_{AA} + I_{BB})$ and $2I_{BA}/(I_{AA} + I_{BB})$. As can be seen from supporting Table SI, such spectra are those recorded at mixing times of 10, 15, 17.5, and 22.5 ms. Because the studied NOE involves two single protons, the intensity of individual cross-peaks ideally should always be equal even if chemical exchange or scalar correlation is present.[27] We interpret the differences between the intensities of individual cross-peaks as a measure of error

in the intensity measurements which is caused by baseline imperfections and t_1 noise. The predominantly negative sign of Δ may signify the presence of a small systematic error associated with t_1 noise.

The slope of the NOE buildup curve, taken with the negative sign, corresponds to the rate of NOE buildup. The negative sign has to be taken because in phase-sensitive NOESY experiments positive (same sign as the diagonal) cross-peaks correspond to the negative NOE.[26] The linear least-squares fit to the data shown in supporting Figure S1 yields the rate of NOE buildup of -0.57 ± 0.10 s^{-1} and corresponds to a rotational correlation time $\tau_c = 3.3 \times 10^{-9} \pm 0.5 \times 10^{-9}$ s at the temperature of the measurement, -82 °C.

The latter parameter can also be estimated from the Stokes model as

$$\tau_c = \frac{\eta V}{kT} = \frac{4\pi\eta}{3kT}abc \qquad (11)$$

where a, b, c are the axes of the ellipsoid representing the molecule. This estimate yields $\tau_c = 1.7 \times 10^{-9}$ s^{-1}, which is in fair agreement with the experimental value. The difference can be attributed to polarity of the solvent, the presence of the Cl$^-$ anion, solvation of both ions, and the fact that the molecule of interest neither is extremely large as compared to the solvent molecules nor has the shape of a sphere. In fact, TMP complex **3** has "cavities" that may accommodate solvent molecules and potentially increase the molecular reorientation time.

NOE buildup measurements have also been attempted at the 300 MHz magnetic field strength (CD$_2$Cl$_2$, -80 °C), but the low intensity of the cross-peaks under these conditions makes a quantitative interpretation unreliable. Indeed, at 300 MHz complex **3** is even closer to the crossover from the positive NOE to the negative NOE than it is at 500 MHz; therefore, the intensity of NOE cross-peaks is intrinsically lower at 300 MHz. While this improves the accuracy of exchange rate measurements,[7] it greatly increases the error of NOE buildup rate measurements. However, our observation was that the NOE between the two pyrrole protons is also negative at the 300 MHz field at -80 °C. This is consistent with the value of the rotational correlation time obtained at 500 MHz.

NOEs in Complexes 1 and 2. A number of NOESY experiments have been performed in this study in attempts to detect NOEs between pyrrole protons in complexes **1** and **2**. The probed conditions included 300 and 500 MHz field strengths, various temperatures (20, -35, -60 °C), and various mixing times (usually ranging from 0.5 to 2 times the pyrrole protons T_1 at the respective temperature). Steady-state experiments have also been performed at the 500 MHz field strength at -60 °C.

None of these experiments have indicated the existence of NOEs between any pair of pyrrole protons in complexes **1** and **2**. Such an outcome was not expected by us and is contrary to the results reported in ref 4 from this research group, where an NOE between protons b and c was reported for both complexes, as well as an NOE between protons a and d in complex **2** at 300 MHz, at -35 °C in CD$_2$Cl$_2$. The ^{1}H spectral assignments based on the apparent connectivities observed in the NOESY spectra appear to be consistent with the chemical shift pattern predicted from the shape of the calculated frontier molecular orbitals. In particular, good agreement was observed between the chemical shift values of pyrrole protons and the spin densities on the adjacent carbon atoms.[4]

On the other hand, serious consideration has to be given to the fact that the original NOESY spectra[4] were recorded and processed in the magnitude mode, which introduces the problem of twisted-phase line shapes, which is removed by the magnitude calculation. This, and the shifted sinebell apodization used, broaden the diagonal peaks significantly, and overlapping tails from the diagonal peaks can be easily mistaken for a cross-peak.

It was also unexplained how such spatially distant protons as (a) and (d) in complex **1** (>7 Å) should exhibit an NOE. The cross-peaks observed between these protons could potentially originate from a phenomenon different from the nuclear Overhauser effect, and therefore it seemed important that the system be analyzed theoretically and the theoretical predictions compared to the previous[4] experimental results.

Predicting the Sign, the Absolute Value, and the Detectability of an NOE. The above comparison of the experimental and the theoretically estimated rotational correlation time τ_c demonstrates that it is possible to estimate the rotational correlation time with a reasonable accuracy from the Stokes model and to subsequently estimate the rate of interproton cross-relaxation if information such as the solvent viscosity,[53] the molecular size, and the interproton distance is available.

It also shows a way to estimate in what temperature range one can expect to find cross-peaks between pyrrole protons. Let us assume that "detectable" cross-peaks are those with relative intensity of 0.01 or larger (by the absolute value) when detected at mixing times smaller than twice the T_1 (called here the critical mixing time). Such an assumption is justified by the following two experimental observations: (i) cross-peaks of a lower intensity are likely to be covered by t_1 noise from their respective diagonal peaks to an extent preventing their accurate integration; (ii) a spectrum recorded at longer mixing times is likely to have such a small absolute signal intensity that spectral noise would significantly distort the measured peak volumes.

Let us also assume that the Stokes formula can yield a rotational correlation time that is within a factor of 2 of the actual correlation time. That is,

$$\tau_c{}^{actual} = \xi\tau_c{}^{Stokes} \qquad 0.5 \leq \xi \leq 2 \qquad (12)$$

If functional approximations for the solvent viscosity and the T_1s as functions of temperature are available, one can evaluate the maximum achievable relative intensity of NOE cross-peaks as a function of temperature and the random parameter ξ which is used to account for the random error in correlation time estimates.

An example of such a plot is shown in Figure 5. The relative intensity of cross-peaks between the pyrrole protons at the mixing time equal to the shorter of the two T_1s is plotted there as a function of temperature, T, and the random parameter ξ. It is important to realize that functional approximations for the viscosity and T_1s have been used to create the plot, rather than their fixed values. The functional approximations do not have to conform to any particular physical model, but they need to reflect, with reasonable accuracy, the values of the corresponding parameters at a given temperature.

If, for a given temperature, the relative intensity of a cross-peak is larger than an arbitrary 1% threshold for all values of ξ, then such cross-peak should be considered potentially detectable at that temperature. The detectability is questionable if only some values of ξ give satisfactory relative cross-peak intensities. Finally, if no values of T or ξ give a satisfactory intensity of the cross-peaks, then the NOE should be considered undetectable.

Such plots have been constructed for all pairs of protons in complexes **1**−**3** that can potentially exhibit NOEs. A summary is presented in Table 2. Our conclusion regarding the matter

Iron(III) Tetraphenylporphyrinates

J. Phys. Chem. A, Vol. 101, No. 49, 1997 **9215**
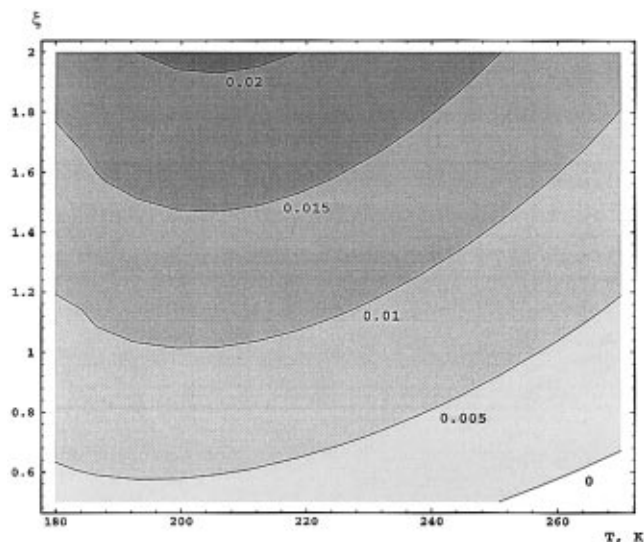
Figure 5. A contour map predicting the detectability of NOE between protons b and c of complex **3** in CD_2Cl_2. The horizontal axis shows the temperature; the vertical axis is an arbitrary factor ξ explained in the text accompanying eq 12. The map shows the relative intensity of NOE cross-peaks at the mixing time equal to the shortest of the two T_1s at a given temperature. The optimum detection temperature on this map is approximately 200 K. It is assumed that the axial ligands are frozen, and therefore chemical exchange does not make it impossible to detect the NOE at the higher temperatures. Similar plots can be constructed for any system with known molecular geometry and temperature dependences of the T_1s and the solvent viscosity.

TABLE 2: Estimated Minimum T_1 Needed for NOE To Be Detectable in CD_2Cl_2 at -77 °C, 500 MHz[a]

complex	protons	r, Å	min T_1, s	actual T_1, s	detectable?	detected?[b]
TMP	b−c	2.61	0.008	0.044	yes	yes
TMP	a−b, c−d	5.28	0.6	0.035	no	no
TPP	b−c	5.41	0.9	0.009	no	no
TPP	a−b, c−d	2.62	0.009	0.009	perhaps	no

[a] Rotational correlation time 3.3×10^{-9} s, detectability limit of 1% of the diagonal peak intensity, and critical mixing time of $2T_1$ are used. [b] Under the experimental conditions of this study (solvent CD_2Cl_2, 500 MHz, temperature -82 °C).

is that the only detectable NOEs in complexes **1** and **2** can be those between protons a, b and c, d, although even those NOEs are on the threshold of detectability. These NOEs have not been detected by the authors of this work, although it is possible that they may be detectable on a gradient instrument with low t_1 noise or in a more viscous solvent.

Regarding the proton pairs b, c and a, d in complexes **1** and **2**, it is the authors' confident conclusion that these NOEs are undetectable. Qualitatively, during the mixing time required for these NOEs to build up the pyrrole protons completely relax, and therefore no NOEs for these protons can be observed in a NOESY spectrum. The cross-relaxation rate can be increased by choosing a different solvent or temperature, but it is highly improbable that such increase could be sufficient for the NOEs to build up within the critical mixing time.

Although we do not have an explanation as to the nature of NOESY cross-peaks detected in ref 4, two scenarios can potentially be involved: (i) the described cross-peaks are the product of overlapping diagonal peaks, which may be likely considering the resolution in the indirect dimension and the magnitude mode under which the spectra were acquired; (ii) the cross-peaks may originate from a phenomenon different from NOE, although at this time we cannot suggest any particular mechanism of their appearance, and we have not been able to

detect them under any of our experimental conditions. In either case, they cannot originate from the actual nuclear Overhauser effect, a conclusion supported by the experimental and theoretical findings of this work.

Concluding Remarks. In this work, we have investigated the temperature dependence of NMR parameters (chemical shifts, T_1s and T_2s) in three different paramagnetic metalloporphyrin complexes and utilized their behavior to explain the experimentally observed NOESY spectra of each complex. We have demonstrated that chemical shifts as well as relaxation times in all three compounds represent the intrinsic values of these parameters only at low temperatures, while at high temperatures they are modified by chemical exchange. From the NOE buildup curve constructed for one of the complexes, we determined the value of its molecular rotational correlation time and found it to be in fair agreement with the theoretical prediction obtained from the Stokes model. We also show how to use the obtained relaxation and NOE buildup data to find the optimal temperature for recording NOESY spectra that involve an NOE between two structurally rigid protons and to predict whether the NOE between a particular pair of structurally rigid protons is observable in NOESY spectra. The latter method was developed here for paramagnetic metalloporphyrin complexes but is general enough to be extended to any compound in which the temperature dependence of the T_1s for the protons in question is known.

Supporting Information Available: Table of relative intensities of cross-peaks between pyrrole protons b and c in **3** and figures of NOE buildup curves as well as a sample NOESY spectrum of **3** (4 pages). Ordering information is given on any current masthead page.

References and Notes

(1) Barbush, M.; Dixon, D. W. *Biochem. Biophys. Res. Commun.* **1985**, *129*, 70.

(2) Yu, C.; Unger, S. W.; La Mar, G. N. *J. Magn. Reson.* **1986**, *67*, 346.

(3) Keating, K. A.; de Ropp, J. S.; La Mar, G. N.; Balch, A. L.; Shiau, F.-Y.; Smith, K. M. *Inorg. Chem.* **1991**, *30*, 3258.

(4) Tan, H.; Simonis, U.; Shokhirev, N. V.; Walker, F. A. *J. Am. Chem. Soc.* **1994**, *116*, 5784.

(5) Nakamura, M.; Groves, J. T. *Tetrahedron* **1988**, *44*, 3225.

(6) Walker, F. A.; Simonis, U. *J. Am. Chem. Soc.* **1991**, *113*, 8652.

(7) Shokhirev, N. V.; Shokhireva, T. Kh.; Polam, J. R.; Watson, C. T.; Raffii, K., Simonis, U.; Walker, F. A. *J. Phys. Chem. A* **1997**, *101*, 2778.

(8) Shokhireva, T. Kh.; Nesset, M. J. M.; Walker, F. A. *Inorg. Chim. Acta*, in press.

(9) Shokhirev, N. V.; Walker, F. A. *J. Phys. Chem.* **1995**, *99*, 17795.

(10) *NMR of Paramagnetic Molecules*; La Mar, G. N., Horrocks, Jr., W. DeW., Holm, R. H., Eds.; Academic Press: New York, 1973.

(11) Drago, R. S. *Physical Methods for Chemists*; Saunders College Publishing: London, 1992.

(12) Banci, L.; Bertini, I.; Luchinat, C. *Nuclear and Electronic Relaxation*; VCH: Weinheim, 1991.

(13) (a) Solomon, I. *Phys. Rev.* **1955**, *99*, 559. (b) Bloembergen, N.; Morgan, L. O. *J. Chem. Phys.* **1961**, *34*, 842. (c) Unger, S. W.; Jue, T.; La Mar, G. N. *J. Magn. Reson.* **1985**, *61*, 448.

(14) (a) McConnell, H. M. *J. Chem. Phys.* **1956**, *24*, 764. (b) Unger, S. W.; Jue, T.; La Mar, G. N. *J. Magn. Reson.* **1985**, *61*, 448.

(15) (a) Gueron, M. *J. Magn. Reson.* **1975**, *19*, 58. (b) Vega, A. J.; Fiat, D. *Mol. Phys.* **1976**, *31*, 347.

(16) Abragam, A. *Principles of Nuclear Magnetism;* Oxford University Press: Oxford, 1961.

(17) See: Jesson, J. P. *The Paramagnetic Shift in NMR of Paramagnetic Molecules*; G. N., La Mar, W. DeW., Horrocks, Jr., R. H., Holm, Eds.; Academic Press: New York, 1973 and references therein.

(18) (a) Walker, F. A.; Balke, V. L.; McDermott, G. A. *Inorg. Chem.* **1982**, *21*, 3342. (b) Walker, F. A.; Balke, V. L.; McDermott, G. A. *J. Am. Chem. Soc.* **1982**, *104*, 1569.

(19) (a) Nesset, M. J. M. Ph.D. Thesis, University of Arizona, 1994. (b) Nesset, M. J. M.; Shokhireva, T. Kh.; Shokhirev, N. V.; Jacobson, S. E.; Walker, F. A. Manuscript in preparation.

(20) (a) *Felix User Guide*, version 2.3; Biosym Technologies: San Diego, 1993. (b) *Felix Command Language Reference Guide*, version 2.3; Biosym Technologies: San Diego, 1993.

(21) *Aspect 3000 NMR Software Manual*; Bruker: 1986.

(22) Vold, R. L.; Waugh, J. S.; Klein, M. P.; Phelps, D. E. *J. Chem. Phys.* **1968**, *48*, 3831.

(23) Güntert, P.; Wüthrich, K. *J. Magn. Reson.* **1992**, *96*, 403.

(24) *Sigma-Plot*, version 5.00;; Jandel Scientific: Corte Madera, CA, 1986−1992.

(25) Hahn, E. L. *Phys. Rev.* **1950**, *80*, 580.

(26) Bodenhausen, G.; Kogler, H.; Ernst, R. R. *J. Magn. Reson.* **1984**, *58*, 370.

(27) Ernst, R. R.; Bodenhausen, G.; Wokaun, A. *Principles of Nuclear Magnetic Resonance in One and Two Dimensions*; Claredon Press: Oxford, 1987.

(28) Higgins, T. B.; Safo, M. K.; Scheidt, W. R. *Inorg. Chim. Acta* **1990**, *178*, 261.

(29) Momot, K. I.; Walker, F. A. *J. Phys. Chem. A* **1997**, *101*, 2787.

(30) Polam, J. R.; Shokhireva, T. Kh.; Raffii, K.; Simonis, U.; Walker, F. A. *Inorg. Chim. Acta*, in press.

(31) La Mar, G. N.; Walker, F. A. *J. Am. Chem. Soc.* **1975**, *97*, 5103.

(32) Walker, F. A.; Benson, M. J. *J. Phys. Chem.* **1982**, *86*, 3495.

(33) La Mar, G. N.; Walker, F. A. *J. Am. Chem. Soc.* **1973**, *95*, 1782.

(34) Simonneaux, G.; Hindre, F.; Le Plouzennec, M. *Inorg. Chem.* **1989**, *28*, 823.

(35) Peyton, D. H.; La Mar, G. N.; Pande, U.; Ascoli, F.; Smith, K. M.; Pandey, R. K.; Parish, D. W.; Bolognesi, M.; Brunori, M. *Biochemistry* **1989**, *28*, 4880.

(36) Walker, F. A.; Simonis, U.; Zhang, H.; Walker, J. M.; Ruscitti, T. M.; Kipp, C.; Amputch, M. A.; Castillo, B. V.; Cody, S. H.; Wilson, D. L.; Graul, R. E.; Young, G. J.; Tobin, K.; West, J. T.; Barichievich, B. A. *New J. Chem.* **1992**, *16*, 609.

(37) Smith, G. M. *Biochemistry* **1979**, *18*, 1628.

(38) McDonald, C. C.; Phillips, W. D. *Biochemistry* **1973**, *12*, 3170.

(39) Ångstrom, J.; Moore, G. R.; Williams, R. J. P. *Biochim. Biophys. Acta* **1982**, *703*, 87.

(40) Timkovich, R.; Cork, M. S.; Taylor, P. V. *Biochemistry* **1984**, *23*, 3526.

(41) Santos, H.; Turner, D. L. *Magn. Reson. Chem.* **1993**, *31*, S90.

(42) Horrocks, W. D.; Greenberg, E. S. *Biochim. Biophys. Acta* **1973**, *322*, 38.

(43) Horrocks, W. D.; Greenberg, E. S. *Mol. Phys.* **1974**, *27*, 993.

(44) Poe, M.; Phillips, W. D.; Glickson, J. D.; McDonald, C. C.; San Pietro, A. *Proc. Natl. Acad. Sci. U.S.A.* **1971**, *68*, 68.

(45) Turner, D. L. *Eur. J. Biochem.* **1993**, *211*, 563.

(46) Basu, P.; Shokhirev, N. V.; Enemark, J. H.; Walker, F. A. *J. Am. Chem. Soc.* **1995**, *117*, 9042.

(47) (a) Allerhand, A.; Gutowsky, H. S. *J. Chem. Phys.* **1964**, *41*, 2115. (b) Allerhand, A.; Gutowsky, H. S. *J. Chem. Phys.* **1965**, *42*, 1587.

(48) (a) Forsen, S.; Hoffman, R. A. *J. Chem. Phys.* **1963**, *39*, 2892. (b) Forsen, S.; Hoffman, R. A. *J. Chem. Phys.* **1964**, *40*, 1189. (c) Forsen, S.; Hoffman, R. A. *J. Chem. Phys.* **1966**, *45*, 2049. (d) Luz, S.; Meiboom, S. *J. Chem. Phys.* **1964**, *40*, 2686.

(49) Momot, K. I.; Walker, F. A. Manuscript in preparation.

(50) La Mar, G. N.; Walker, F. A. *J. Am. Chem. Soc.* **1973**, *95*, 6950.

(51) Banci, L.; Bertini, I.; Luchinat, C. *Magn. Reson. Rev.* **1986**, *11*, 1.

(52) (a) Bothner-By, A. A.; Stephens, R. L.; Lee, J.; Warren, C. D.; Jeanloz, R. W. *J. Am. Chem. Soc.* **1984**, *106*, 811. (b) Bax, A.; Davis, D. G. *J. Magn. Reson.* **1985**, *63*, 207.

(53) Perry, J. H. *Chemical Engineers' Handbook*, 5th ed.; McGraw-Hill: New York, 1973.